

FATIGUE CRACK GROWTH RATE (FCGR) BEHAVIOR OF NICALON/SiC COMPOSITES – N. Miriyala, P. K. Liaw, N. Yu and C. J. McHargue (University of Tennessee), L. L. Snead (Oak Ridge National Laboratory) and D. K. Hsu (Iowa State University).

OBJECTIVE

To develop a fundamental understanding of fatigue crack growth phenomenon in Nicalon/SiC composites.

SUMMARY

Ultrasonic measurements were continued on the Nicalon/SiC composite specimens to correlate elastic moduli with percentage porosity in the in-plane as well as through-thickness directions. A micromechanics model based on periodic microstructure was developed to predict the elastic stiffness constants of the Nicalon/SiC composites. The predicted values were in good agreement with the experimental results.

PROGRESS AND STATUS

Introduction

Ceramic matrix composites (CMCs) are attractive candidate materials for high-temperature structural applications because of their low density and ability to withstand higher temperatures and more aggressive environments than most metals or other conventional engineering materials [1-3]. Although CMCs are now being considered seriously for many potential structural applications, they can be susceptible to degradation under cyclic fatigue loading, even when such loading is fully compressive. However the field of "fatigue in ceramics" is still in its infancy and much work is yet to be done to understand the mechanical behavior of fiber reinforced ceramic matrix composites [4]. In view of the above, it has been decided to study the fatigue crack propagation behavior of Nicalon/SiC composites processed by the Forced Chemical Vapor Infiltration (FCVI) technique, using the ASTM standard E 647-92 for the measurement of fatigue crack growth rate in metallic materials.

Nicalon/SiC composites processed by the FCVI technique have a fabric lay-up of [0-30/30-120/60-150]_n. From earlier work [5] it was observed that there are two major types of porosity in the Nicalon/SiC composites, viz., porosity between the fiber tows and interlaminar porosity. Also, the composite is highly anisotropic and, therefore, it is only to be expected that the mechanical properties of the material will vary significantly along different directions and with different levels of densification. These effects are inherent from the fabrication process used to manufacture the composite material.

Compliance measurements are widely used to measure the crack length as well as characterize the near crack tip field phenomena during monotonic and fatigue crack growth testing. However, the elastic modulus of each sample has to be known to permit the use of the technique. In view of the variation in density values, and consequently moduli values from specimen to specimen, and also to develop an indirect method for measuring the moduli values, ultrasonic measurements were made on the specimens.

Apart from being able to experimentally measure the mechanical properties of the composites, it is also necessary to develop theoretical models to predict the properties of the composite material from the knowledge of the properties of the constituents (fiber and matrix) that we already know. However, there have been only a very few attempts so far to predict the moduli of woven fabric composites [6]. Hence, it was decided to develop a theoretical model to predict the elastic stiffness constants of the Nicalon/SiC composites. A homogenization method was used in the analysis, wherein it is possible to transform a heterogeneous unit cell of the composite material into a homogeneous one comprising of the matrix only, prescribing stress-free (eigen) strains.

Ultrasonic Measurements

Based on acoustic wave theory [7,8] the elastic stiffness constant (C) can be expressed as a function of ultrasonic velocity as

$$C = \rho * V^2 \dots\dots\dots(1)$$

Where ρ = density of the material,
 V = Ultrasonic Velocity

From longitudinal and shear wave ultrasonic velocity measurements we can estimate the elastic stiffness constants of the material using equation (1). Longitudinal measurements were performed by 'dry coupling' to avoid possible contamination by the couplant. A 'pulse-echo overlap method' was used to measure the wave velocities. A schematic of the experimental setup for longitudinal measurements is shown in Figure 1. The reference signal is obtained by passing ultrasonic waves through a reference test system comprised of a rubber sheet and a fused quartz piece. The test sample is then placed between the transmitting transducer and the rubber sheet reference test system and ultrasonic waves are passed through the setup. The signals are received by the receiving transducer and captured by an oscilloscope. The signal peaks from the reference test system, with and without the presence of sample, are matched as closely as possible, and from the phase shift between the two the time taken by the ultrasonic waves to travel through the sample is measured. The thickness of the sample divided by the time taken for the ultrasonic waves to pass through the sample is taken as the ultrasonic velocity through the sample. Since the two signals are matched as closely as possible (i.e. overlapped), this technique is referred to as the pulse-echo overlap method.

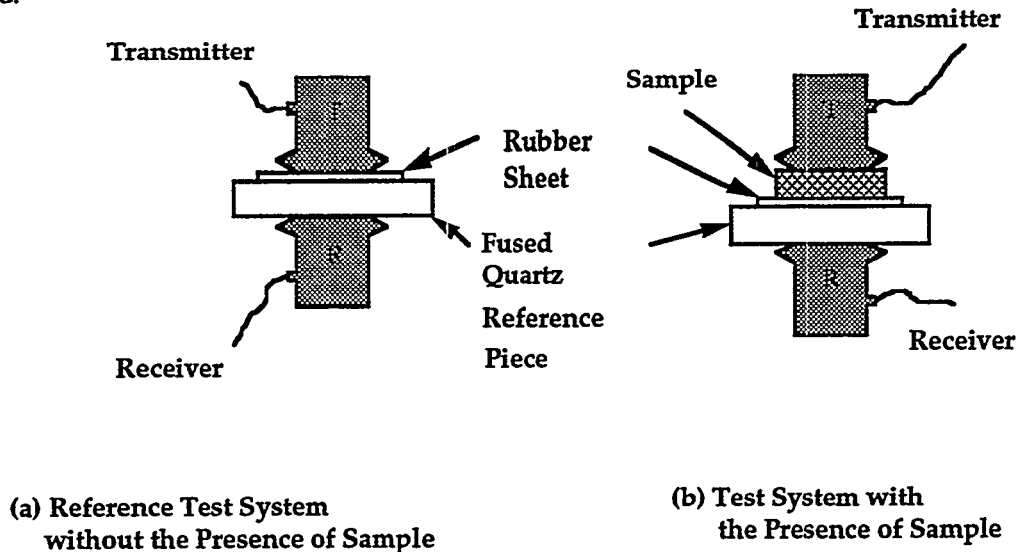


Figure 1. Ultrasonic Measurement Setup

Longitudinal wave measurements were made in the in-plane as well as through-thickness orientations. For the shear wave velocity measurements the same setup as in Figure 1 was employed except that the rubber sheet was eliminated and regular contact mode shear wave transducers were coupled with burnt honey. Honey was also used for the coupling between the sample and the reference quartz plate. Because the shear couplant was highly viscous and the area fraction of surface breaking voids on the in-plane surfaces was much less than that on the edges, the effect on velocity due to couplant-filled voids was believed to be small. In this setup the shear wave propagated through the sample in the thickness direction and the polarization direction was in-plane. The polarization vectors of the two transducers were aligned with aligned with each other but not to any particular fiber direction in the plane of the composite laminate.

The density of the samples varied from 2.06 to 2.63 g/cm³ and the porosity from 11.5 to 30.4%. The longitudinal and shear moduli values are plotted against percent porosity in Figures 2 and 3. It is apparent from Figures 2 and 3 that porosity has a dramatic effect on lowering the moduli values of the composites. From Figure 2 it can also be seen that the longitudinal moduli in the in-plane direction (129 to 248 GPa) were greater than in the through-thickness direction (5.6 to 138.2 GPa), as is to be expected from the fabric lay-up. Shear moduli values of the composites (9.9 to 57.9 GPa) were much lower than the longitudinal moduli values (Figure 3).

Theoretical Modeling

A micromechanics model based on periodic microstructure was developed to estimate the effect of porosity on the elastic properties of the Nicalon/SiC composites. As shown in Figure 4, a representative unit cell, which is repeated in all directions, consists of eight woven fiber tows in the shape of elliptic cylinders and one parallelepiped that is used to model the interlaminar porosity.

When the infinite composite with a periodic microstructure is subjected to a homogeneous strain field, ϵ^0 , due to the existence of periodically distributed fibers and voids, the resulting stress and strain fields are $\sigma^0 + \sigma^P(x_1, x_2, x_3)$ and $\epsilon^0 + \epsilon^P(x_1, x_2, x_3)$, where σ^0 and ϵ^0 are homogeneous (average) stresses and strains, σ^P and ϵ^P the periodic disturbance stress and strain fields, respectively. The elastic moduli of the composite are defined by Equation (2).

$$\{\sigma^0\} = [\bar{C}]\{\epsilon^0\} \dots\dots\dots(2)$$

Based on Eshelby's [9] concept of transformation strain, one can replace the porous heterogeneous unit cell by a homogeneous cell comprised of matrix material only and prescribe stress-free strains in the fibers (Ω_1) and voids (Ω_2) such that the average stress and average strain fields remain the same everywhere in the unit cell before and after the homogenization. That is, the following consistency conditions [Equation (3)] must hold:

$$\begin{aligned} [C^{\Omega_1}]\{\epsilon^0 + \langle \epsilon^P \rangle_{\Omega_1}\} &= [C^M]\{\epsilon^0 + \langle \epsilon^P \rangle_{\Omega_1} - \epsilon^{*1}\} && \text{in } \Omega_1 \dots\dots\dots 3(a) \\ [C^{\Omega_2}]\{\epsilon^0 + \langle \epsilon^P \rangle_{\Omega_2}\} &= [C^M]\{\epsilon^0 + \langle \epsilon^P \rangle_{\Omega_2} - \epsilon^{*2}\} && \text{in } \Omega_2 \dots\dots\dots 3(b) \end{aligned}$$

where the angle brackets with the subscript Ω_1 (Ω_2) represent the volume average over Ω_1 (Ω_2); C^{Ω_1} , C^{Ω_2} (= 0), and C^M are the stiffness of fibers, voids, and matrix, respectively; ϵ^{*1} and ϵ^{*2} are the stress-free homogenization strains prescribed in fibers and voids and are approximated by distinct constants. The average periodic disturbance strains can be related to the stress-free strains [10] by

$$\langle \epsilon^P \rangle_{\Omega_\alpha} = [\hat{\Gamma}][C^M] \sum_{n_1, n_2, n_3}^{\pm\infty} (f_{\Omega_1} g_1 g_\alpha \{\epsilon^{*1}\} + f_{\Omega_2} g_2 g_\alpha \{\epsilon^{*2}\}) \text{ for } \alpha = 1, 2 \dots\dots\dots(4)$$

where the term $(n_1, n_2, n_3) = (0,0,0)$ is excluded in the summation, and the components of the fourth-order tensor, Γ , are given by

$$\begin{aligned} \hat{\Gamma} &= \frac{1}{G^M} \left(\xi_\alpha^2 - \frac{1}{2(1-\nu^M)} \xi_\alpha^4 \right) \text{ for } \alpha = 1, 2, 3 \\ \hat{\Gamma}_{\alpha\beta} &= \hat{\Gamma}_{\beta\alpha} = \frac{-1}{2G^M(1-\nu^M)} \xi_\alpha^2 \xi_\beta^2 \text{ for } (\alpha, \beta) = (1, 2), (2, 3), (3, 1) \end{aligned}$$

$$\hat{\Gamma}_{\alpha\alpha} = \frac{1}{G_M} \left(\frac{1}{4} (\xi_\beta^2 + \xi_\gamma^2) - \frac{1}{2(1-\nu^M)} \xi_\beta^2 \xi_\gamma^2 \right)$$

for $(\alpha, \beta, \gamma) = (4, 2, 3), (5, 3, 1), (6, 1, 2)$

$$\hat{\Gamma}_{\alpha\beta} = 0 \quad \text{otherwise}$$

and

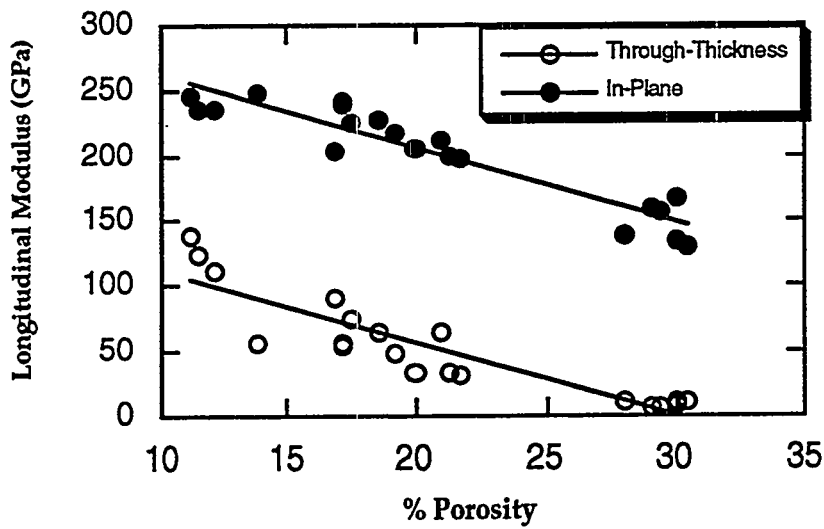


Figure 2. Longitudinal Moduli vs. % Porosity in Nicalon/SiC Composites

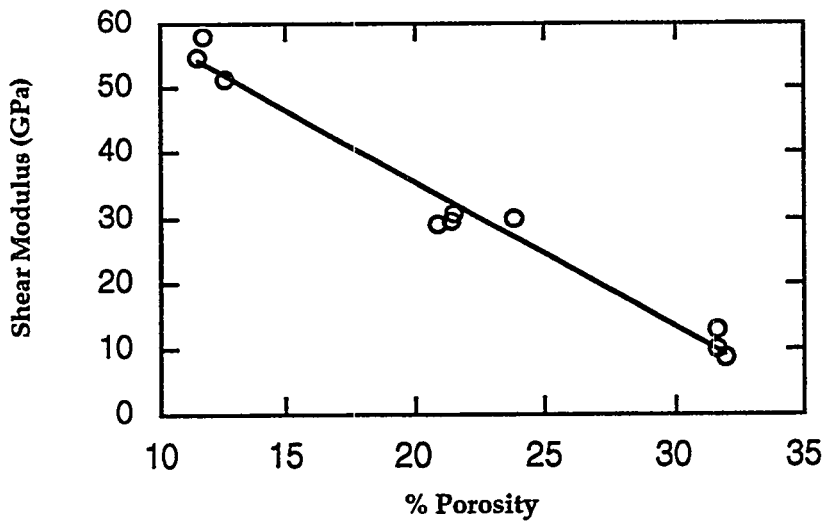


Figure 3. Shear Moduli vs. % Porosity in Nicalon/SiC Composites

$$\xi_i = \frac{n_i}{a_i \sqrt{\left(\frac{n_1}{a_1}\right)^2 + \left(\frac{n_2}{a_2}\right)^2 + \left(\frac{n_3}{a_3}\right)^2}} \quad \text{for } i = 1, 2, 3;$$

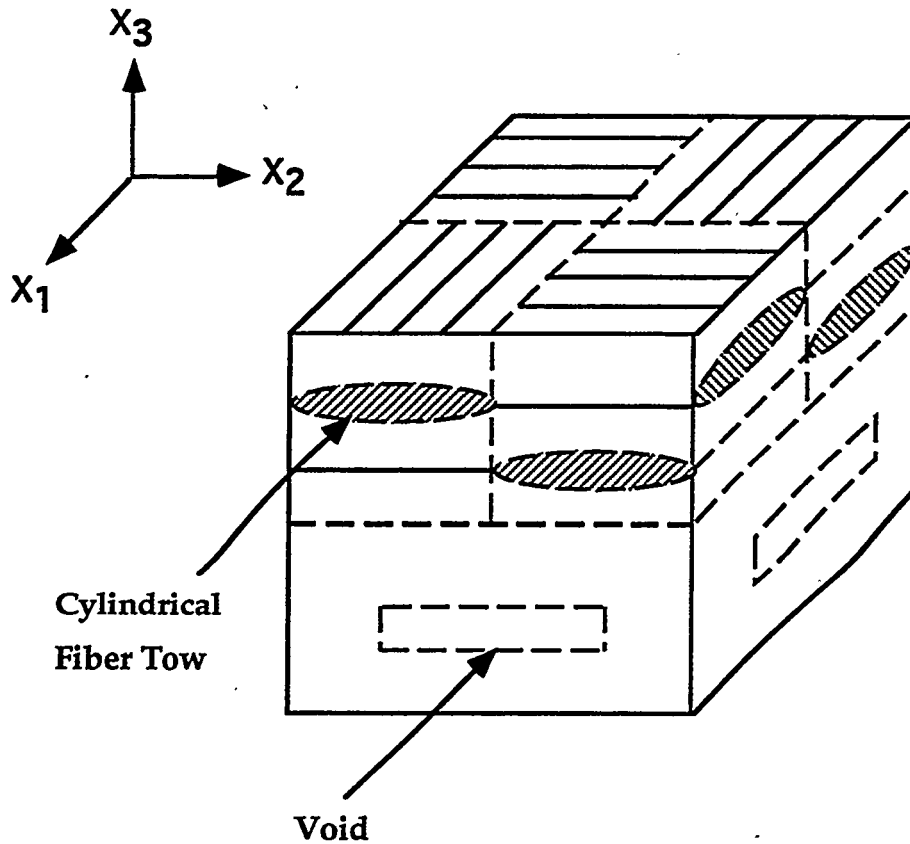


Figure 4. A Model Based on Periodic Microstructure

G^M and ν^M are the shear modulus and Poisson's ratio of the matrix; a_i ($i=1, 2, 3$) are the dimensions of the unit cell; n_i are integers; f_{Ω_1} and f_{Ω_2} are fiber and void volume fractions, respectively. The shape and size of the fibers and voids are accounted for in g_1 and g_2 . For elliptic-cylindrical fiber tows,

$$g_1 = \frac{1}{2} \cos\left(\frac{\pi n_1}{2}\right) \cos\left(\frac{\pi n_2}{2}\right) \cos\left(\frac{\pi n_3}{4}\right) \cos\left(\frac{\pi n_3}{2}\right) (g_A + g_B)$$

where

$$g_A = \frac{2 \sin\left(\frac{\pi n_2 c_2}{a_2}\right) J_1\left(\pi \sqrt{\left(\frac{n_1 c_1}{a_1}\right)^2 + \left(\frac{n_3 c_3}{a_3}\right)^2}\right)}{\left(\frac{\pi n_2 c_2}{a_2}\right) \left(\pi \sqrt{\left(\frac{n_1 c_1}{a_1}\right)^2 + \left(\frac{n_3 c_3}{a_3}\right)^2}\right)}$$

$$\text{and } g_B = \frac{2 \sin\left(\frac{\pi n_1 c_1}{a_1}\right) J_1\left(\pi \sqrt{\left(\frac{n_2 c_2}{a_2}\right)^2 + \left(\frac{n_3 c_3}{a_3}\right)^2}\right)}{\left(\frac{\pi n_1 c_1}{a_1}\right) \left(\pi \sqrt{\left(\frac{n_2 c_2}{a_2}\right)^2 + \left(\frac{n_3 c_3}{a_3}\right)^2}\right)}$$

with c_1 (or c_2) and c_3 being the principal radii of the elliptic cross-section and c_2 (or c_1) the length of the cylinder; J_1 is the Bessel function of the first kind. For a parallelepiped,

$$g_2 = \cos\left(\frac{n\pi_3}{2}\right) \frac{\sin\left(\frac{\pi n_1 b_1}{a_1}\right) \sin\left(\frac{\pi n_2 b_2}{a_2}\right) \sin\left(\frac{\pi n_3 b_3}{a_3}\right)}{\left(\frac{\pi n_1 b_1}{a_1}\right) \left(\frac{\pi n_2 b_2}{a_2}\right) \left(\frac{\pi n_3 b_3}{a_3}\right)}$$

where b_1 , b_2 and b_3 are the dimensions of the parallelepiped.

After solving the consistency conditions for suitable ε^{*1} and ε^{*2} , which preserve the same stress and strain fields before and after homogenization, the elastic moduli of the porous woven-fabric composites are thus determined by Equation (5).

$$[\bar{C}]\{\varepsilon^o\} = [C^M]\left(\{\varepsilon^o\} - f_{\Omega_1}\{\varepsilon^{*1}\} - f_{\Omega_2}\{\varepsilon^{*2}\}\right) \dots\dots\dots(5)$$

To calculate the moduli of the composites, the following input data were used [11]; the shear modulus and Poisson's ratio of the NicalonTM fiber were 80 GPa and 0.12, respectively, and those of the matrix were 146 GPa and 0.2. The predicted values are plotted in Figure 5 along with the experimental results. It can be seen that there is an excellent agreement between the theoretically predicted values and measured elastic moduli.

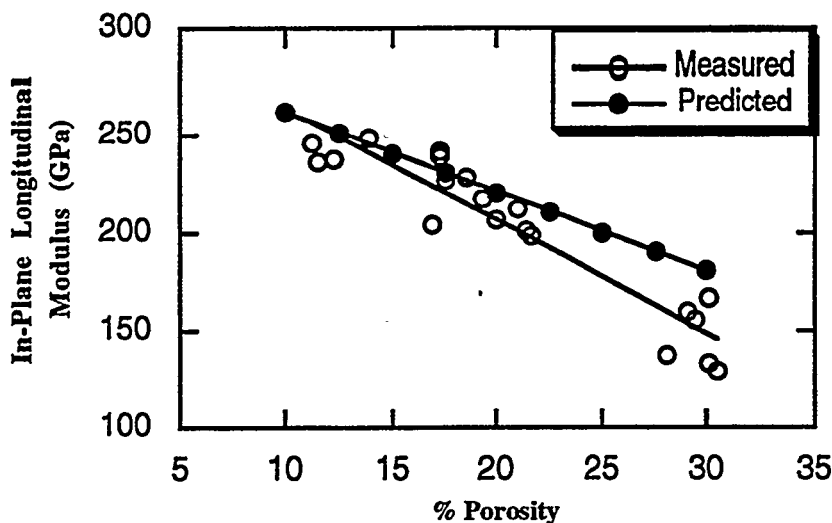


Figure 5. Comparison of Predicted and Measured In-Plane Longitudinal Moduli

FUTURE WORK

- (i) Fatigue crack growth testing of the C(T) specimens under different loading conditions at ambient as well as elevated temperatures.
- (ii) Fractography of the specimens to assess the various damage and crack shielding mechanisms that govern the fatigue and fracture behavior of the Nicalon/SiC composites.

ACKNOWLEDGMENTS

This work is supported by the Department of Energy under contract No. Martin Marietta 11X-SL261V to the University of Tennessee. We are grateful to Dr. Arthur Rowcliffe and Dr. Everett Bloom of ORNL for their continued encouragement and support in our endeavors.

REFERENCES

- [1] K. K. Chawla, *Ceramic Matrix Composites* (Chapman & Hall, London, 1993) pp. 4-10.
- [2] J. A. DiCarlo, *Adv. Mater. & Proc.*, 135 (June 1989) 41.
- [3] T. M. Besmann, B. W. Sheldon, R. A. Lowden and D. P. Stinton, *Science*, 253 (1991) 1104.
- [4] R. H. Duaskardt, R. O. Ritchie and B. N. Cox, *Advanced Materials and Processes*, 144 (August 1993) 30.
- [5] P. K. Liaw, D. K. Hsu, N. Yu, N. Miriyala, V. Saini, H. Jeong and K. K. Chawla, *Proc. Int. Symp. on High Performance Composites: Commonality of Phenomena*, Rosemont, Illinois, USA, October 2-6, 1994, eds. K. K. Chawla, P. K. Liaw and S. G. Fisherman (TMS, Warrendale, 1994) 377.
- [6] N. J. Fang and T. S. Chou, *J. Am. Ceram. Soc.*, 76 (1993) 2539.
- [7] H. Jeong, D. K. Hsu, R. E. Shannon and P. K. Liaw, *Metallurgical Transactions A*, 25 A (1994) 799.
- [8] H. Jeong, D. K. Hsu, R. E. Shannon and P. K. Liaw, *Metallurgical Transactions A*, 25 A (1994) 811.
- [9] J. D. Eshelby, *Proc. R. Soc. London*, A241 (1957) 376.
- [10] S. Nemat-Nasser, N. Yu, and M. Hori, *Mech. Mater.*, 15 (1993) 163.
- [11] J. L. Bohet, Ph. D Thesis, Bordeaux, France, 1993.